Invited Paper

A hybrid antenna coupled Nb_5N_6 microbolometer for dual polarization THz detection

Chengtao Jiang [1], Pengfei Chen [1], Mengxin Liu [1], Chao Wan [2], Xuecou Tu [1*, 2], Xiaoqing Jia [1, 2], Lin Kang [1, 2], Jian Chen [1, 2], and Peiheng Wu [1, 2]
[1] Research Institute of Superconductor Electronics (RISE), School of Electronic Science and Engineering, Nanjing University, Nanjing 210023, China
[2] Purple Mountain Laboratories, Nanjing 211111, China
[*1] Email: tuxuecou@nju.edu.cn

(Received March 2022)

Abstract: A hybrid antenna coupled Nb_5N_6 microbolometer was demonstrated for dual polarization terahertz (THz) THz detection. By adding a ring resonant antenna (RRA) in another vertical direction and optimizing the structure of the hybrid antenna, the electric field intensity at the center of the antenna was maximized in both horizontal and vertical polarization directions, and the corresponding electric field at 0.193 *THz* were 60 *V/m* and 65 *V/m*, respectively. The hybrid antenna coupled Nb_5N_6 microbolometer THz detector was prepared. The measurement results verify the dual polarization characteristics of the detector. The maximum voltage responsivity of the antenna coupled detector in the horizontal direction at 0.198 *THz* was roughly the same as the vertical direction at 0.202 *THz*. While the voltage responsivity of the Nb_5N_6 microbolometer detector without RRA in the vertical polarization direction was 2.75 *times* larger than that of the horizontal direction. These results clearly show that the hybrid antenna coupled Nb_5N_6 microbolometer detector has the advantage of improving the voltage responsivity in the other direction, and thus realizing dual polarization THz detection. It has great potential applications in the field of the THz security inspection and spectral imaging.

Keywords: Nb_5N_6 microbolometer, THz detection, Dual polarization

doi:

1. Introduction

THz wave is an electromagnetic wave with frequencies ranging from 0.1 to 10 *THz* and wavelength ranging from 3 *mm* to 30 μm, which is between the microwave and infrared frequencies in the electromagnetic spectrum [1]. Because of the particularity of its band, it has the characteristics of both electronics and photonics, not only covering the vibration and rotation frequencies of many biological macromolecules [2], but also including the low-energy excitation frequency band of electronic materials [3]. Meanwhile, THz wave can penetrate non-polar materials such as ceramics, plastics, carbon plates, clothing and fat with very small attenuation [4-7]. Therefore, THz wave has great application prospects in the fields of astronomy [8], information communication [9], atmospheric remote sensing [10], medical imaging [11], life sciences [12], security inspection [13] and so on. At the same time, many contraband and dangerous explosives can be accurately distinguished by their "fingerprint spectrum" in the THz band. Therefore, the THz imaging in detecting concealed inflammable, explosive, metal weapons and drugs is of great significance [14]. The bolometers for both direct and mixer detection are usually used to perform security inspection on the human body and hidden objects. The radiation of the human body and the hidden objects have complex polarization characteristics, which are related to the geometric structure of the human body or objects, the dielectric constant of internal medium and the spatial distribution of temperature [15, 16]. However, most of the bolometers can only detect a single polarization information [17-20]. Therefore, a large amount of polarization information of objects will be lost if a single polarization bolometer is used, and the information of the hidden objects can not be accurately identified during security inspection.

In this paper, a ring resonant antenna (RRA) was added in the vertical direction of the dipole antenna, this hybrid antenna coupled Nb_5N_6 microbolometer with dual polarization for THz detection was presented. The core unit of the THz detector is a suspended Nb_5N_6 thin film microbridge [21-24], which can reduce the heat conduction between the Nb_5N_6 thin film and the Si substrate, thereby improving the sensitivity of the detector. The hybrid antenna is designed on a Si substrate with a Fabry–Pérot (FP) cavity. The hybrid antenna was designed and optimized by using the electromagnetic simulation software, and the best electric field intensity at the center of the antenna in both horizontal and vertical polarization directions was realized, and the corresponding electric field intensity are 60 *V/m* and 65 *V/m*, respectively. The measurement results show that the optical voltage responsivities of the detector with RRA are almost the same in the horizontal and vertical directions, which are in good agreement with the simulation results.

2. Design and fabrication of RRA coupled Nb_5N_6 microbolometer

The geometry of the hybrid antenna coupled Nb_5N_6 microbolometer is depicted in Fig. 1 (a). It consists of a dipole antenna, a ring resonant antenna in the orthogonal direction, two bias electrodes and a Nb_5N_6 film microbridge. The two electrodes with the size of 200 μm×200 μm are used to provide bias current for the Nb_5N_6 microbolometer. The antenna is placed on a thermally oxidized silicon substrate with a period of 1000×1000 μm^2, and the Nb_5N_6 microbolometer is at the feed point of the antenna. The thickness of the Si substrate, the thermal SiO_2 on the Si surface and antenna layer (Au film) are 540 μm, 200 *nm* and 200 *nm*, respectively. A 200 *nm* thick Au layer is provided on the backside of the Si substrate as a reflect mirror to further enhance the coupling efficiency of the antenna to the THz signals. In the simulation model in CST, the X and Y directions are both set as periodic boundary conditions, and the ±Z directions are both set as open boundary conditions. The electric field monitor Probe is placed at the center of the gap to detect the electric field intensity of the antenna, as shown in Fig.1 (b). The plane wave excitation is set up to simulate the normal incidence of uniform plane wave irradiating on the antenna. The electric field of the incident plane THz wave ($\boldsymbol{E_0}$) is set E_0 = 1 *V/m* and the direction of it is along the -Z direction. The electric field of the incident THz wave parallel to the X axis is defined as

$\boldsymbol{E}\angle 0°$, and the electric perpendicular to the X axis field is defined as $\boldsymbol{E}\angle 90°$.

To maximize the electric field intensity in both horizontal and vertical directions, and realize dual polarization detection for the microbolometer, the hybrid antenna was optimized as follow: first, when the electric field of the incident linearly polarized THz wave parallel to the X axis ($\boldsymbol{E}\angle 0°$), the length of Au wires (L) between the Nb_5N_6 film microbridge and the electrode is optimized. The calculated electric field (E) normalized to the incident electric field ($\boldsymbol{E_0}$) magnitude at the center of microbridge change with L, as shown in Fig. 1 (c). The electric field increases first and then decreases with L. When L = 220 μm, the maximum resonance electric field reaches up to 62 V/m at 0.193 THz. when the electric field of the incident linearly polarized THz wave perpendicular to the X axis ($\boldsymbol{E}\angle 90°$), the calculated relationship between the electric field and the L is shown in Fig. 1 (d). The electric field also changes with L, and it is similar to the results in the other direction ($\boldsymbol{E}\angle 0°$). Results show that the maximum electric field is enhanced by a factor of 58 at 0.193 THz. We chose L = 200 μm as the optimized length for the best electric field at the center of the hybrid antenna in both horizontal and vertical directions. Then, we investigated the influence of the angel of the RRA (θ in Fig. 1 (a)) on the resonance characteristics and the electric field intensity at the center of the hybrid antenna when L = 200 μm. Fig. 1 (e) shows that the electric field at the center of the antenna change with θ when L = 200 μm and $\boldsymbol{E}\angle 0°$. As the value of θ becomes larger, the E increases first and then decreases. The electric field reaches the maximum value of 60 V/m at θ = 60° at 0.193 THz. However, at $\boldsymbol{E}\angle 90°$, the electric field increases with θ, as shown in Fig. 1 (f). The electric field increases from 53 V/m to 93 V/m when θ increases from 50° to 80°. Thus θ = 60° is the best choice considering the electric field in both horizontal and vertical directions. The electric field at the center of the antenna is 65 V/m when $\boldsymbol{E}\angle 90°$ and θ = 60° at 0.193 THz. Therefore, considering comprehensively, we chose L = 200 μm, θ = 60°, R = 160 μm and W_1 = W_2 = 20 μm as the optimal parameters of the target antenna. Fig. 1 (g) and (h) show the electric field distribution of the optimized hybrid antenna coupled microbolometer detector in the X-Z and Y-Z planes. It shows that the electric field is mainly concentrated in the central area of the hybrid antenna, that is, the area where the Nb_5N_6 film microbridge is located. This means that the received energy at the detector is significantly enhanced, so as to improve the voltage responsivity of the detector.

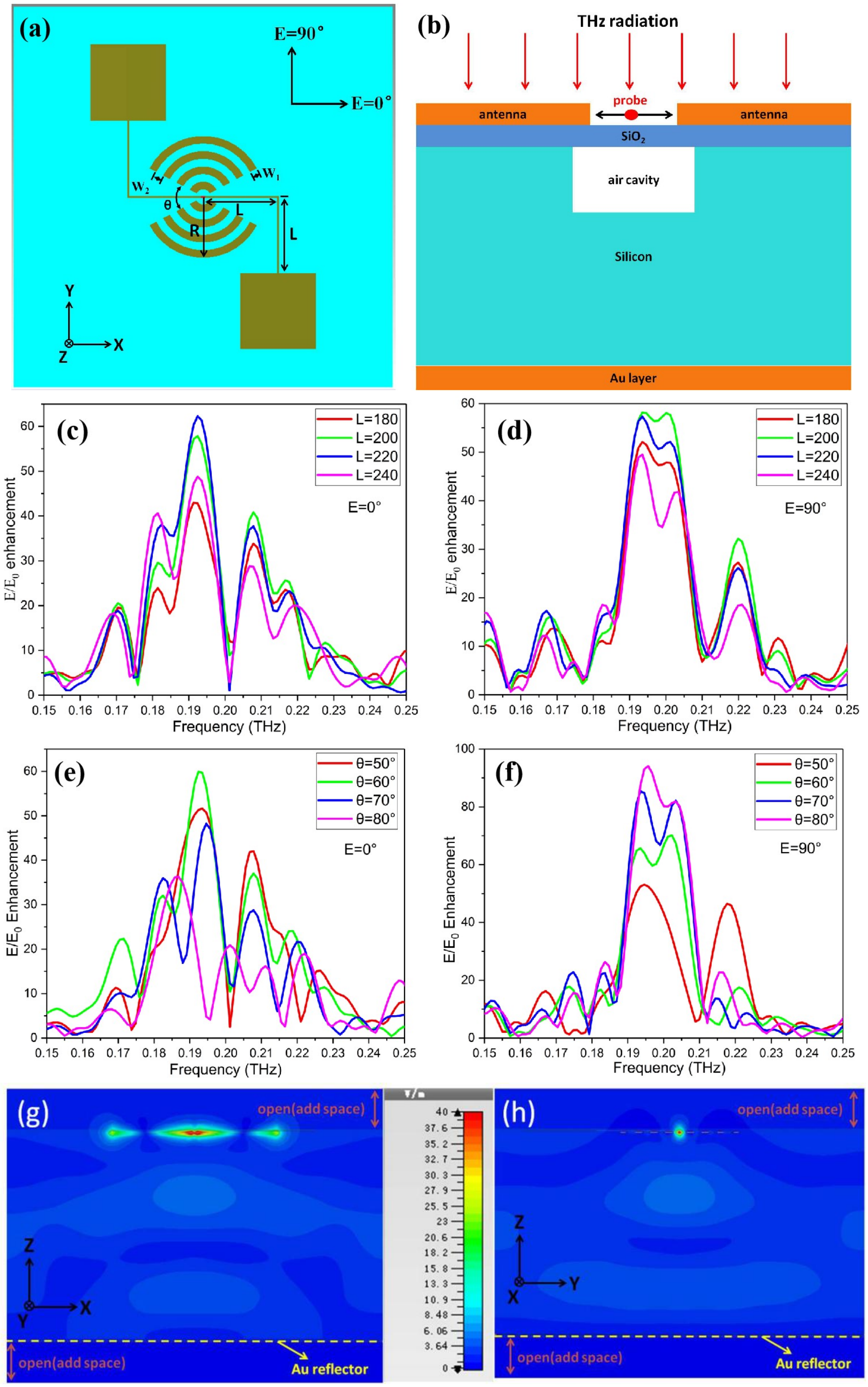

Fig. 1 (a) Schematic diagram of the hybrid antenna designed for the dual polarization Nb_5N_6 microbolometer detector. (b) Cross-sectional view of the antenna coupled Nb_5N_6 microbolometer. The electric field enhancement factor (***E*/*E₀***) at the center of the hybrid antenna for different L when $\boldsymbol{E}\angle 0°$ (c) and $\boldsymbol{E}\angle 90°$ (d). The electric field enhancement factor ($\boldsymbol{E}/\boldsymbol{E_0}$) changes with the value of θ when $\boldsymbol{E}\angle 0°$ (e) and $E\angle 90°$ (f) at L = 200 μm. The calculated distribution of $\boldsymbol{E}$ in the X-Z plane (g) and Y-Z plane (h) for the antenna coupled detector at 0.193 *THz*.

The antenna coupled microbolometers with or without the RRA are prepared, and the optical micrographs are shown in Fig. 2. The fabrication process in details could be found in our previous work [25], and special attention should be paid to the preparation of the air bridge of the microbolometer, which requires very fine etching conditions. These two type microbolometers are fabricated on the same silicon substrate, and all dimensions are the same except for the RRA. The hybrid antenna coupled Nb_5N_6 microbolometers are shown in Fig. 2 (a). The Nb_5N_6 film microbridge which is supported by the SiO_2 layer is suspended in the air is enlarged from Fig. 2 (a) and shown in Fig. 2(b). Fig. 2(c) and (d) show the Nb_5N_6 microbolometers without RRA and its suspended Nb_5N_6 film microbridge, respectively.

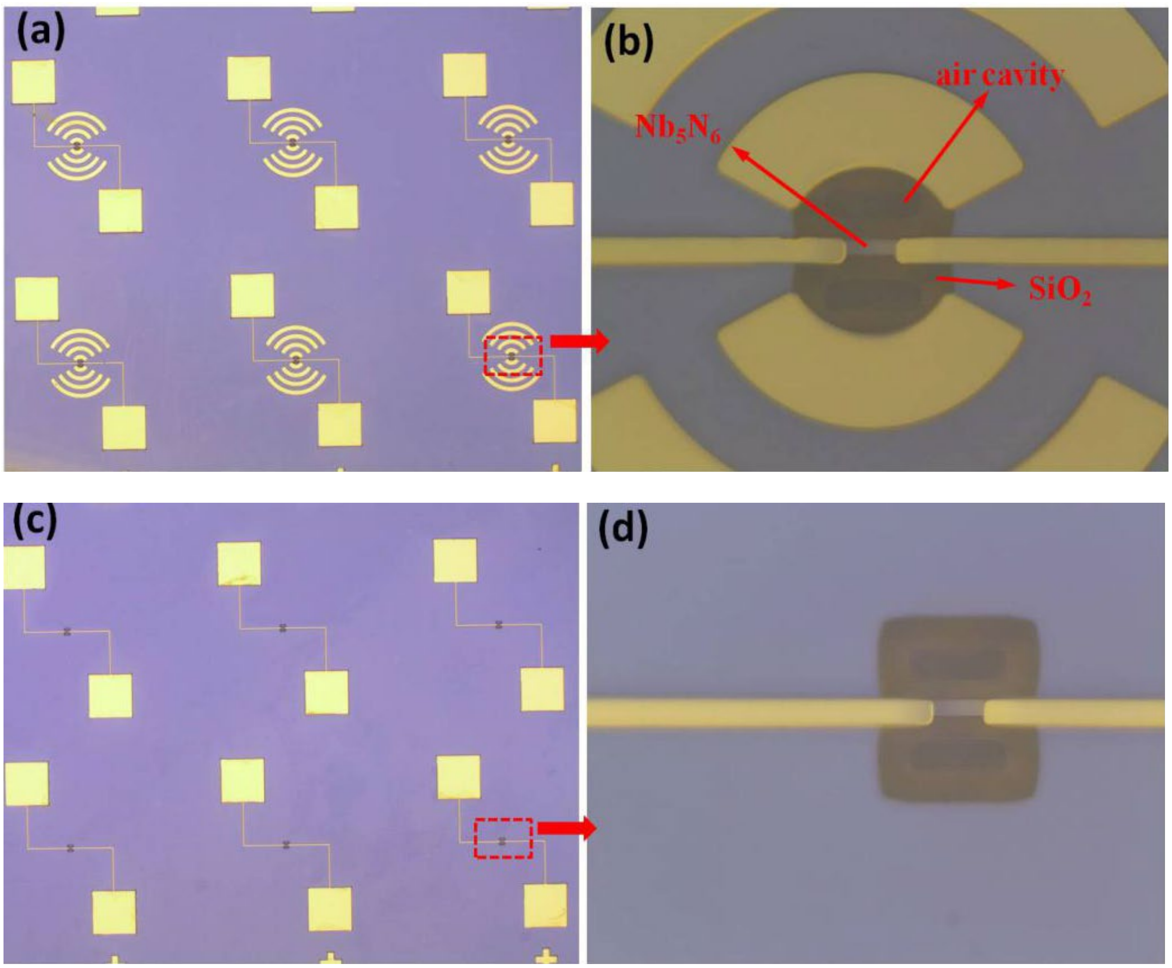

Fig. 2 Optical micrographs of the fabricated Nb_5N_6 microbolometers integrated with/without the RRA and the enlarged display for the suspended Nb_5N_6 film microbridges.

3. Characterization of the hybrid antenna coupled Nb_5N_6 microbolometer

A. Setup for the Nb_5N_6 microbolometer polarization measurement

Figure 3 depicts the measurement setup for the Nb_5N_6 microbolometer polarization characterization. The THz source used is composed of AMC-336 frequency multiplier produced by VDI company and Agilent E8251D signal generator. To obtain a THz signal in the range of 0.17-0.25 *THz*, a low frequency signal (9.4-13.8 *GHz*) provided by the signal generator was amplified by the AMC-336 multiplier (18 *times*). The polarization of the electric field of the incident THz wave was labeled in Fig. 3. The modulation frequency of the THz signal is 1 *kHz*, and which is also the reference signal of the lock-in amplifier (SR830). By using two off-axis parabolic (OAP) mirrors, the THz beam is focused on the Nb_5N_6 microbolometer which is connected to the read-out circuit. When the Nb_5N_6 microbolometer receives the THz signals, the resistance of the Nb_5N_6 film changes due to thermal effect of the thermistor, and then a corresponding change in the voltage of the microbolometer is produced under a given bias current. The value of the voltage is read out by the lock-in amplifier and then collected by the computer, thus the readout voltage represents the incident THz power. To measure the polarization of the detector, the device is first fixed with the RRA in the vertical to the direction of the electric field of the incident THz wave, and the measured optical voltage responsivities at this time is marked as $\boldsymbol{E}\angle 0°$. Then, the detector was rotated by 90°, and the optical voltage responsivities is marked as $\boldsymbol{E}\angle 90°$. Finally, all the measured data are normalized and plotted in Fig. 4.

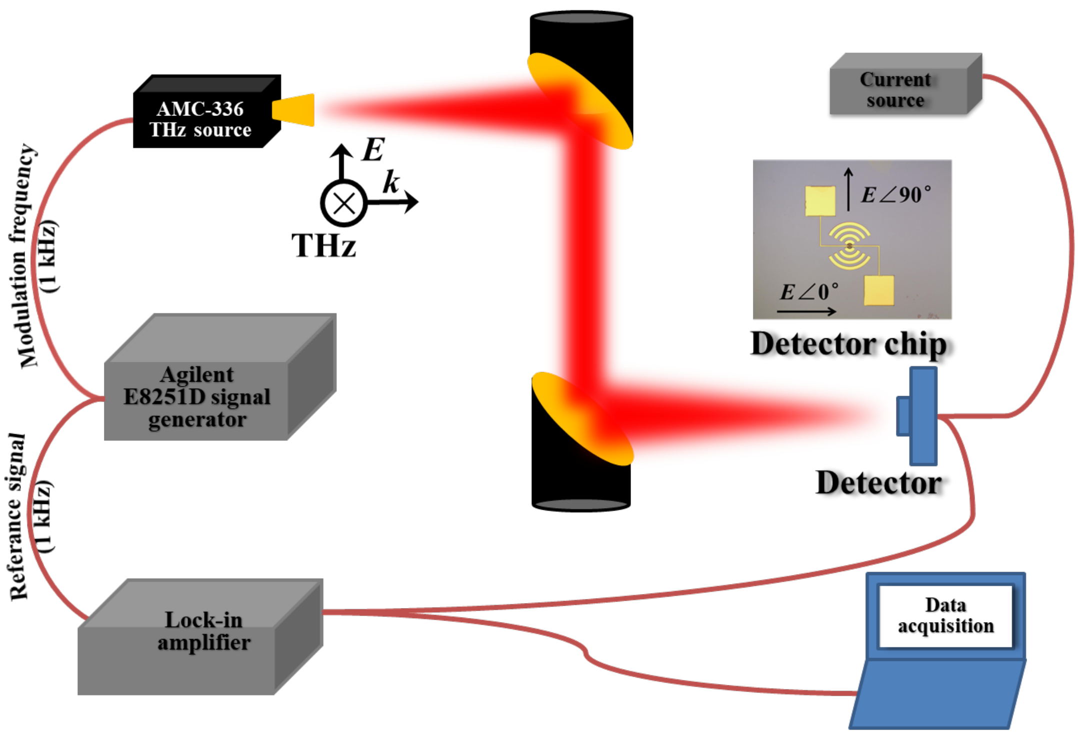

Fig. 3 Setup for the Nb_5N_6 microbolometer polarization measurement.

B. The measured polarization of the Nb_5N_6 microbolometer

Fig. 4 (a) shows the measured optical responsivity of the hybrid antenna coupled Nb_5N_6 microbolometer in horizontal and vertical direction from 0.17 *THz* to 0.25 *THz*. The optical responsivity is defined

$$R_V = \frac{V_{out}}{P_f}$$

V_{out} is the readout voltage of the lock-in amplifier, P_f is the total THz power at the focal plane which is measured by the power meter. To facilitate comparison, the measured voltage responsivities and calculated electric field intensity ($\boldsymbol{E}^2$) are normalized. The measured maximum optical responsivity (red dot line) is at 0.205 *THz*, there is a little deviation from the calculated results (blue line) by the simulation at $\boldsymbol{E}\angle 90°$, and the measured maximum optical responsivity (green dot line) in the horizontal direction ($\boldsymbol{E}\angle 0°$) is at 0.198 *THz*, and is 90% of the maximum optical responsivity at $\boldsymbol{E}\angle 90°$, there is also a little deviation from the calculated 0.192 *THz* by the simulation as shown in gray line in Fig. 4 (a). The difference between the measured best optical responsivities at the two orthogonal directions is only 10%. In general, the results of the measured optical responsivities and the calculated electric field intensities at the detector are in good agreement. This slight difference may come from the micromachining error and the structural parameters set in the simulation. To further illustrate the polarization characteristics of the detector, we also measured the optical responsivities of the dipole antenna coupled Nb_5N_6 microbolometer without RRA in the above two orthogonal directions, as shown in Fig. 4 (b). The measured maximum optical responsivity (blue dot line) in the vertical direction ($\boldsymbol{E}\angle 90°$) is at 0.204 *THz*, and is 2.75 *times* that in the horizontal direction ($\boldsymbol{E}\angle 0°$). It obviously reveals the single polarized characteristic of the detector without RRA. It is worth noting that an resonant peak appears at 0.215 *THz* in both of the Nb_5N_6 microbolometers when the polarization of the electric field of the incident THz wave is in the horizontal direction ($\boldsymbol{E}\angle 0°$). However, the corresponding resonant peaks are not obvious in the vertical direction ($\boldsymbol{E}\angle 90°$) as shown in Fig. 4 (a) and (b). This phenomenon may be caused by the accumulation of electrical charges at the corners of Au lead wires, as shown in Fig. 1(g).

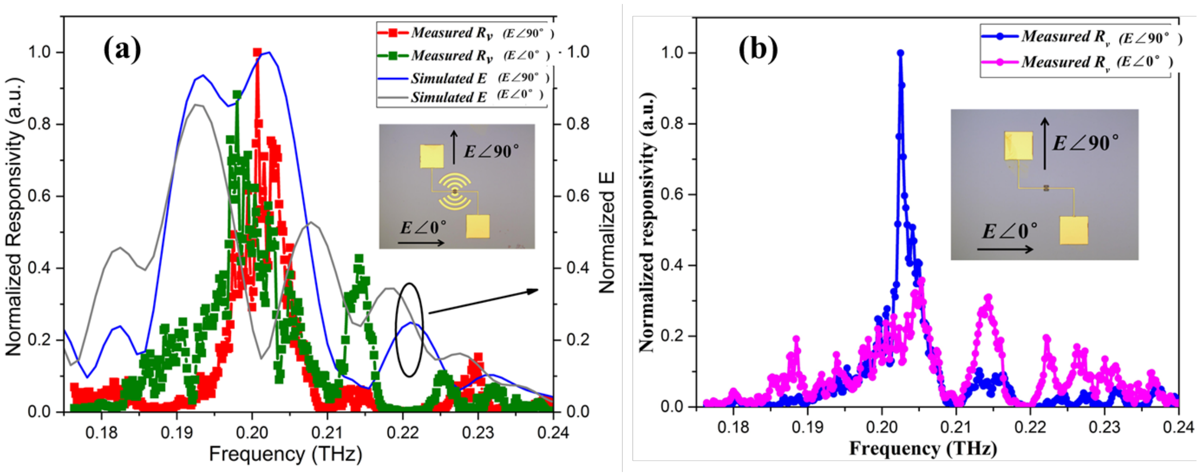

Fig. 4 (a). The measured optical voltage responsivities of the antenna coupled Nb_5N_6 microbolometers with RRA in the two orthogonal directions ($\boldsymbol{E}\angle 0°$ and $\boldsymbol{E}\angle 90°$). The calculated electric field (a.u.) at the hybrid coupled Nb_5N_6 microbolometer in $\boldsymbol{E}\angle 0°$ and $\boldsymbol{E}\angle 90°$. (b) The measured optical voltage responsivities of the antenna coupled Nb_5N_6 microbolometers without RRA in the two orthogonal directions ($\boldsymbol{E}\angle 0°$ and $\boldsymbol{E}\angle 90°$).

5. Conclusions

A hybrid antenna coupled Nb_5N_6 microbolometer was demonstrated for dual polarization THz detection. The calculated electric field at the center of the antenna are 60 *V/m* and 65 *V/m* at 0.193 *THz* in $\boldsymbol{E}\angle 0°$ and $\boldsymbol{E}\angle 90°$, respectively. The Nb_5N_6 microbolometers with/without RRA are prepared. The measured results verified the detector with the RRA has the ability of dual polarization detection, which are consistent with the calculated results. In addition, the optical responsivity of the detector without RRA in $\boldsymbol{E}\angle 0°$ is 2.75 *times* higher than that in $\boldsymbol{E}\angle 90°$. The hybrid antenna coupled Nb_5N_6 microbolometer has great potential applications in security inspection and imaging.

Acknowledgments

This research was supported by the Key Technologies Research and Development Program (2018YFB1801504); National Natural Science Foundation of China (61521001 and 61801209); Fundamental Research Funds for the Central Universities; and Jiangsu Key Laboratory of Advanced Techniques for Manipulating Electromagnetic Waves.

References

[1] Siegel P. H. “Terahertz technology”. *IEEE Trans Microw Theory*. 50 (3): 910-928(2002).

[2] Feng H, Li F, and Chen TN. “Current situation and future trends for THz-biomedicine”. *J Thz Sci Electron Inf Technol*. 11: 827–835(2013)

[3] Zhao L, Hao YH, and Peng RY. “Advances in the biological effects of terahertz wave radiation”. *Mil Med Res*. 1:26(2014).

[4] Naftaly M, Foulds A P, Stringer M R, et al. “Terahertz transmission spectroscopy of nonpolar materials and relationship with composition and properties”[C]. *international conference on infrared, millimeter, and terahertz waves*, 26 (1): 55-64(2004).

[5] I. Catapano, F. Soldovieri, L. Mazzola, et al.. “THz imaging as a method to detect defects of aeronautical coatings”. *J. Infrared, Millim. Terahertz Waves*, 38, 1264-1277(2017)

[6] F. Destic, C. BouvetImpact damages detection on hybrid materials by THz imaging. Case Stud. Nondestruct. Test. Eval., 6, pp. 53-62 (2016)

[7] Wahaia F, Valusis G, Bernardo L M, et al. “Detection of colon cancer by terahertz techniques”[J]. *Journal of Molecular Structure*, 1006(1): 77-82(2011).

[8] Kulesa C. “Terahertz Spectroscopy for Astronomy: From Comets to Cosmology”[J]. *IEEE Transactions on Terahertz Science and Technology*, 1(1): 232-240(2011).

[9] Thomas Kleine-Ostmann, Tadao Nagatsuma. “A Review on Terahertz Communications Research”. *Journal of Infrared, Millimeter, and Terahertz Waves*. ,32, pp.143–171(2011)

[10] J.M. Dai, X.F. Lu, J. Liu, et al.. “Remote THz Wave Sensing in Ambient Atmosphere”. *Terahertz Science and Technology*,Vol.2, No.4, December (2009).

[11] Humphreys K, Loughran JP, Gradziel M, et al. “Medical applications of terahertz imaging: a review of current technology and potential applications in biomedical engineering”. Conf Proc IEEE Eng Med Biol Soc. 2004; 1302-1305(2004).

[12] Yukio Kawano. Terahertz waves: a tool for condensed matter, the life sciences and astronomy, Contemporary Physics, 54:3, pp.143-165(2013)

[13] Michael C. Kemp, P. F. Taday, Bryan E. Cole, et al.. "Security applications of terahertz technology," Proc. SPIE 5070, Terahertz for Military and Security Applications (29 July 2003)

[14] J F Federici, B Schulkin, F Huang, et al.. “THz imaging and sensing for security applications—Explosives, weapons and drugs”. *Semiconductor Science and Technology*, Volume 20, Number 7 (2005.6)

[15] Jalil S Z, Taib M N, Abdullah H, et al.. “Frequency radiation characteristic around the human body”[J]. *International journal of simulation: systems, science and technology*, 12(1): 34-39(2011).

[16] Liboff A R. “Toward an electromagnetic paradigm for biology and medicine”.[J]. *Journal of Alternative and Complementary Medicine*, 10(1): 41-47(2004).

[17] J. Bean, B. Tiwari, G. Szakmany, et al.. “Antenna length and polarization response of antenna-coupled MOM diode infrared detectors”. *Infrared Phys. Technol*., vol. 53, no. 3, pp. 182–185(May 2010).

[18] M. Jestl, I. Maran, A. Köck, et al.. "Polarization-sensitive surface plasmon Schottky detectors". *Opt. Lett.* 14, 719-721 (1989)

[19] Sizov, F. & Rogalski, A. Thz detectors. Prog. Quantum Electron. 34, 278–347 (2010)

[20] Tong J, Muthee M, Chen SY, et al.. "Antenna Enhanced Graphene THz Emitter and Detector". *Nano Lett*. 15(8):5295-5301(2015).

[21] Lu X H, He N, Kang L, et al.. "Nb_5N_6 thin film on silicon and silicon oxide: A good material for terahertz detection"[J]. *Science Bulletin*, 54(18): 3344-3346(2009).

[22] Tu X C, Kang L, Wan C, et al.. "Diffractive microlens integrated into Nb_5N_6 microbolometers for THz detection"[J]. *Optics Express*, 23, 13794-13803(2015).

[23] Tu X, Jiang C, Xiao P, et al.. "Investigation of antenna-coupled Nb_5N_6 microbolometer THz detector with substrate resonant cavity". *Opt Express*. 26(7):8990-8997(2018).

[24] Tu, Xue-Cou, et al.. "Nb_5N_6 Microbolometer Arrays for Terahertz Detection". *Chinese Physics* B, vol. 22, no. 4, p. 40701(2013).

[25] Jiang C, Kang L, Xiao P, et al.. "Influence of periodic structure and pixel area on the performance of antenna‐coupled Nb_5N_6 array detector"[J]. *Microwave and Optical Technology Letters* (2020).